Supplementary Data

Supplementary Materials and Methods

Bending and thrashing assays

To determine the body bend frequency, worms grown for two generations on HT115 expressing the corresponding RNA interference (RNAi) construct were transferred onto a fresh nematode growth medium plate and video recorded for the number of body bends performed in 2 min. A body bend was defined as a change in the direction of the part of the worm corresponding to the posterior bulb of the pharynx along the *y*-axis, assuming that the worm is moving along the *x*-axis (7). To determine the thrashing frequency, worms grown for two generations on HT115 expressing the corresponding RNAi were transferred to a 4 μl M9 drop in a glass-slide. The worms were allowed to settle for 1 min after which the thrashes were video recorded for 2 min. Videos were captured using a SONY CCD camera (model DMK 31AU03) with the ImagingSource software (Imaging Control). Microsoft Excel two-tail Student's *t*-test was used to calculate the *p*-values in the bending and thrashing assays.

Generation of polyclonal antibodies against DNJ-27

The synthetic peptides (NH2–) CKHPDRNTDDPNAHD (–COOH) and (NH2–) CNWKALSEDWEPYNR (–COOH), derived from the *Caenorhabditis elegans* DNJ-27 sequence were conjugated to KLH and used to immunize rabbits (Biomedal). After four immunizations, serum was collected and the polyclonal antibodies were purified by affinity chromatography using a mix of the two peptides.

Supplementary References

1. Calfon M, Zeng H, Urano F, Till JH, Hubbard SR, Harding HP, Clark SG, and Ron D. IRE1 couples endoplasmic reticulum load to secretory capacity by processing the XBP-1 mRNA. *Nature* 415: 92–96, 2002.
2. Cooper AA, Gitler AD, Cashikar A, Haynes CM, Hill KJ, Bhullar B, Liu K, Xu K, Strathearn KE, Liu F, Cao S, Caldwell KA, Caldwell GA, Marsischky G, Kolodner RD, Labaer J, Rochet JC, Bonini NM, and Lindquist S. Alpha-synuclein blocks ER-Golgi traffic and Rab1 rescues neuron loss in Parkinson's models. *Science* 313: 324–328, 2006.
3. Etheridge T, Oczypok EA, Lehmann S, Fields BD, Shephard F, Jacobson LA, and Szewczyk NJ. Calpains mediate integrin attachment complex maintenance of adult muscle in *Caenorhabditis elegans*. *PLoS Genet* 8: e1002471, 2012.
4. Fire A, Xu S, Montgomery MK, Kostas SA, Driver SE, and Mello CC. Potent and specific genetic interference by double-stranded RNA in *Caenorhabditis elegans*. *Nature* 391: 806–811, 1998.
5. Fostel JL, Benner Coste L, and Jacobson LA. Degradation of transgene-coded and endogenous proteins in the muscles of *Caenorhabditis elegans*. *Biochem Biophys Res Commun* 312: 173–177, 2003.
6. Hamamichi S, Rivas RN, Knight AL, Cao S, Caldwell KA, and Caldwell GA. Hypothesis-based RNAi screening identifies neuroprotective genes in a Parkinson's disease model. *Proc Natl Acad Sci U S A* 105: 728–733, 2008.
7. Ikenaka K, Kawai K, Katsuno M, Huang Z, Jiang YM, Iguchi Y, Kobayashi K, Kimata T, Waza M, Tanaka F, Mori I, Sobue G. dnc-1/dynactin 1 Knockdown Disrupts Transport of Autophagosomes and Induces Motor Neuron Degeneration. *PLoS One* 8: e54511, 2013.
8. Link CD. Expression of human beta-amyloid peptide in transgenic *Caenorhabditis elegans*. *Proc Natl Acad Sci U S A* 92: 9368–9372, 1995.
9. Morley JF, Brignull HR, Weyers JJ, and Morimoto RI. The threshold for polyglutamine-expansion protein aggregation and cellular toxicity is dynamic and influenced by aging in *Caenorhabditis elegans*. *Proc Natl Acad Sci U S A* 99: 10417–10422, 2002.
10. Szewczyk NJ, Peterson BK, Barmada SJ, Parkinson LP, and Jacobson LA. Opposed growth factor signals control protein degradation in muscles of *Caenorhabditis elegans*. *EMBO J* 26: 935–943, 2007.
11. Szewczyk NJ, Peterson BK, and Jacobson LA. Activation of Ras and the mitogen-activated protein kinase pathway promotes protein degradation in muscle cells of *Caenorhabditis elegans*. *Mol Cell Biol* 22: 4181–4188, 2002.
12. van Ham TJ, Thijssen KL, Breitling R, Hofstra RM, Plasterk RH, and Nollen EA. *C. elegans* model identifies genetic modifiers of alpha-synuclein inclusion formation during aging. *PLoS Genet* 4: e1000027, 2008.
13. Zdinak LA, Greenberg IB, Szewczyk NJ, Barmada SJ, Cardamone-Rayner M, Hartman JJ, and Jacobson LA. Transgene-coded chimeric proteins as reporters of intracellular proteolysis: starvation-induced catabolism of a lacZ fusion protein in muscle cells of *Caenorhabditis elegans*. *J Cell Biochem* 67: 143–153, 1997.

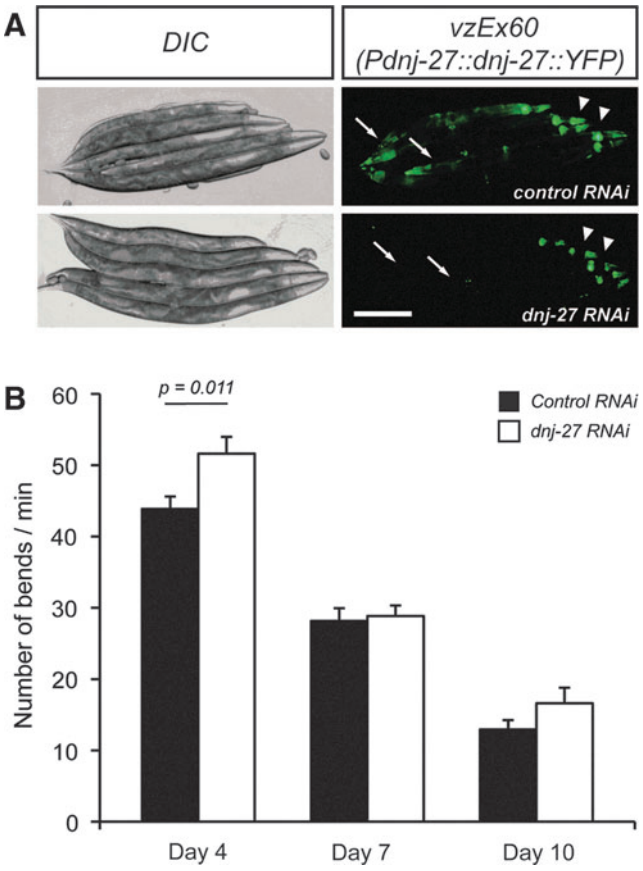

SUPPLEMENTARY FIG. S1. ***dnj-27* RNAi effectiveness and its effect in a bending assay. (A)** Effectiveness of *dnj-27* RNAi measured as decrease of fluorescent signal (*right panel*) in transgenic animals expressing the extrachromosomal array *vzEx60 [Pdnj-27::dnj-27::YFP::KDEL]*. Note that the signal in the intestine (*arrows*) is substantially decreased while in the pharynx area (*triangles*) the effect is less accentuated. Bar = 200 μm. **(B)** Quantification of the body bends associated with forward movement in nematode growth medium plates without food. The results are the average of two independent experiments with 10 animals each. Error bars represent the SEM. RNAi, RNA interference; SEM, standard error of the mean.

A *Quantitative data and statistical analysis of Aβ levels from FIG. 2G immunoblots. (2 independent trials)*

	dvIs2 (Punc-54::Aβ)		
	control RNAi	*dnj-27 RNAi*	*dnj-27 overexp.*
Blot #1 (Aβ / α-tubulin)	1.318116324	0.947677226	0.844646542
Blot #2 (Aβ / α-tubulin)	0.846090935	1.149503741	1.036820145
Mean Aβ content	1.082103629	1.048590483	0.940733344
Standard deviation	0.333772353	0.142712897	0.135887258
SEM	0.236012695	0.100913257	0.096086801
Statistics (unpaired two-tailed t-test)		0.454034459	0.317403402

B *Quantitative data and statistical analysis of α-syn::YFP levels from FIG. 3D immunoblots. (2 independent trials)*

	pkIs2386 (Punc-54::α-syn::YFP)		
	control RNAi	*dnj-27 RNAi*	*dnj-27 overexp.*
Blot #1 (α-syn / α-tubulin)	1.229188207	1.124208293	0.686519941
Blot #2 (α-syn / α-tubulin)	1.190295485	0.753688441	1.384946048
Mean α-syn content	1.209741846	0.938948367	1.035732995
Standard deviation	0.027501308	0.2619971	0.493861836
SEM	0.019446361	0.185259926	0.349213053
Statistics (unpaired two-tailed t-test)		0.141611759	0.334069434

C *Quantitative data of Q40::YFP levels from Supplemental FIG. 4G immunoblots. (1 trial)*

	rmIs133 (Punc-54::Q40::YFP)		
	control RNAi	*dnj-27 RNAi*	*control RNAi*
Blot #1 (Aβ / α-tubulin)	0.915572557	1.271176571	0.851543668

SUPPLEMENTARY FIG. S2. Quantification and statistical analyses of (A) Aβ, (B) α-syn and (C) Q40 worms western blots. The quantification of the blots was performed with the ImageJ Software and the statistical analysis was implemented using the Microsoft Excel Software. α-syn, alpha-synuclein; Aβ, beta amyloid peptide.

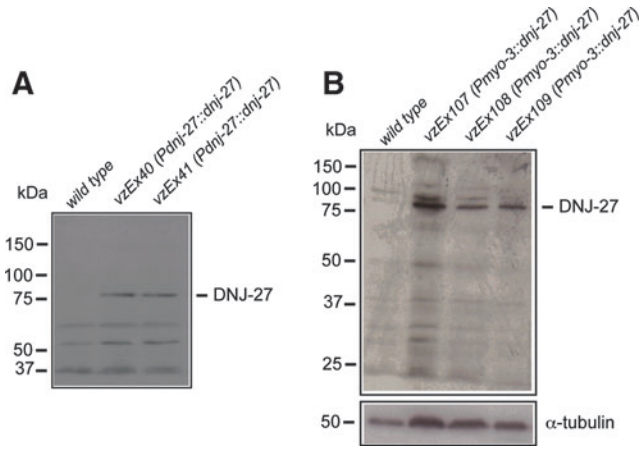

SUPPLEMENTARY FIG. S3. Immunoblot analysis on DNJ-27 overexpressing strains. Immunoblot using polyclonal antibodies against DNJ-27 in N2 wild type control and transgenic strains overexpressing DNJ-27 under the control of its own promoter **(A)** and under the control of the *myo-3* promoter **(B)**. All lanes were loaded with total protein extract from 100 one-day synchronized adults of the corresponding strain. The antibody clearly recognizes the DNJ-27 band about 78 kDa in the transgenic strains, which is barely detectable in the wild type controls. Nonspecific bands at a lower size are used as loading control in (A), while α-tubulin was used as loading control in (B).

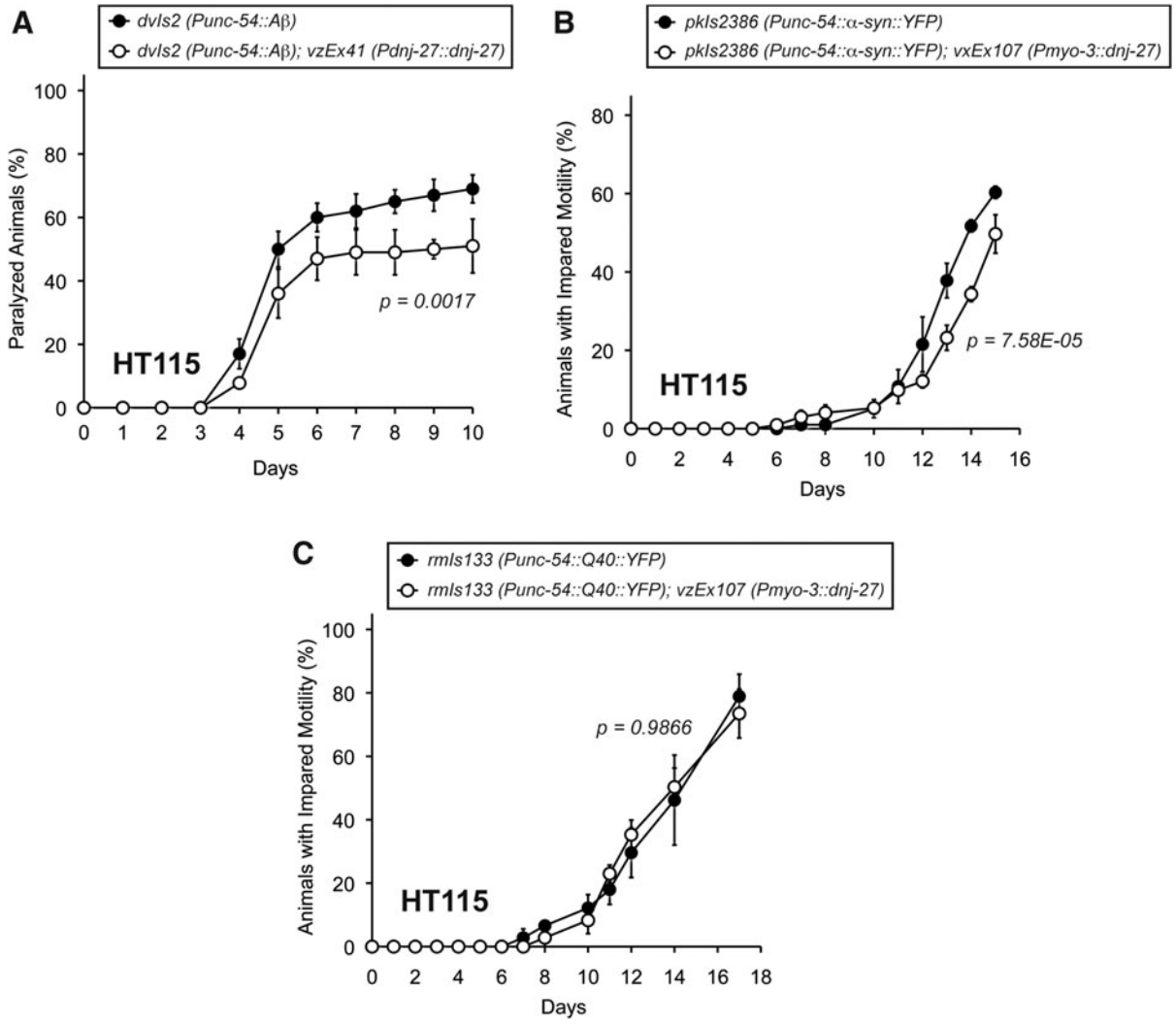

SUPPLEMENTARY FIG. S4. Effect of overexpressing DNJ-27 on Aβ, α-syn and Q40 worms grown on HT-115 bacteria. **(A)** Progressive paralysis of CL2006, *dvIs2 [Punc-54::Aβ3-42::unc-54 3′-UTR; rol-6 (su1006)]* worms (●) and its derivative transgenic strain VZ158 carrying the extrachromosomal array *vzEx41 [Pdnj-27::dnj-27::dnj-27 3′-UTR; Punc-122::GFP]* (○) grown on HT115 bacteria. The graph represents the average of three independent experiments and the error bars indicate the SEM. **(B)** Impaired mobility of NL5901, *pkIs2386 [Punc-54::α-syn::YFP::unc-54 3′-UTR; unc-119 (+)]* worms (●) and its derivative transgenic strain VZ303 carrying the extrachromosomal array *vzEx107 [Pmyo-3::dnj-27 cDNA::unc-54 3′-UTR; Ptrx-3::mCherry]* (○) grown on HT115 bacteria. The graph represents the average of three independent experiments and the error bars indicate the SEM. **(C)** Impaired mobility of AM141, *rmIs133 [Punc-54::Q40::YFP::unc-54 3′-UTR]* worms (●) and its derivative transgenic strain VZ299 carrying the extrachromosomal array *vzEx107 [Pmyo-3::dnj-27 cDNA::unc-54 3′-UTR; Ptrx-3::mCherry]* (○) grown on HT115 bacteria. The graph represents the average of three independent experiments and the error bars indicate the SEM. For statistical analyses, a two-way ANOVA test was performed in all cases. ANOVA, analysis of variance.

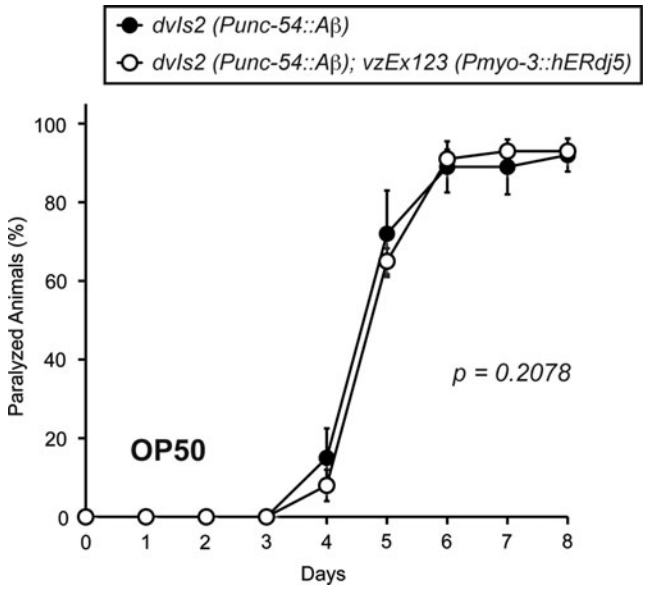

SUPPLEMENTARY FIG. S5. Effect of overexpressing human *ERdj5* on the paralysis phenotype of Aβ worms. Progressive paralysis of CL2006 *dvIs2 [Punc-54::Aβ3-42::unc-54 3′-UTR; rol-6 (su1006)]* worms (●) and its derivative transgenic strain VZ317 carrying the extrachromosomal array *vzEx123 [Pmyo-3::ERdj5::unc-54 3′-UTR; Punc-122::GFP]* (○) grown on OP50 bacteria. The graph represents the average of two independent experiments. The error bars indicate the SEM. Two-way ANOVA was used for the statistical analysis.

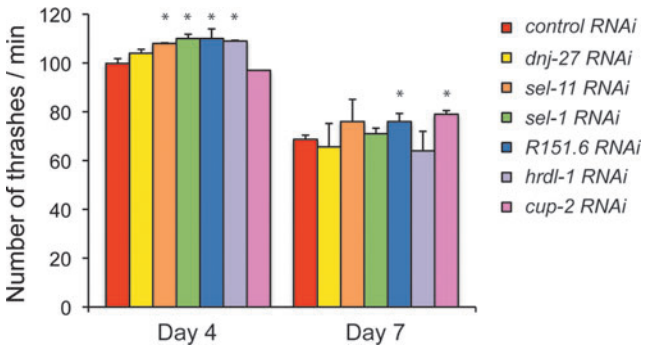

SUPPLEMENTARY FIG. S6. Thrashing assay of wild type *C. elegans* subjected to RNAi of selected endoplasmic reticulum genes. Quantification of the thrashing movements in M9 liquid medium. The results are the average of two independent experiments with 10 animals each. Error bars represent the SEM. For statistical analyses, unpaired *t-test* with two tail distribution was performed. (*$p < 0.05$ with respect to RNAi control).

Supplementary Table S1. Strains Used in This Study

Strain name	*Genotype*	*Reference/source*
	Basic strains	
N2	*Wild type, DR subclone of CB original (Tc1 pattern I)*	CGC[a]
	dnj-27 GFP fusion strains	
BC10640	*dpy-5(e907) I; sEX10640 [rCesY47H9C.5(dnj-27)::GFP + pCeh361]*	CGC
VZ188	*vzEx64 [pVZ34 (Pdnj-27::GFP::unc-54 3′-UTR)]*	This study
VZ189	*vzEx65 [pVZ34 (Pdnj-27::GFP::unc-54 3′-UTR)]*	This study
VZ190	*vzEx66 [pVZ34 (Pdnj-27::GFP::unc-54 3′-UTR)]*	This study
VZ184	*vzEx60 [pVZ378 (Pdnj-27::dnj-27::YFP::KDEL::unc-54 3′-UTR)]*	This study
	dnj-27 overexpression strains	
VZ148	*vzEx40 [pVZ325 (Pdnj-27::dnj-27::dnj-27 3′-UTR); Punc-122::GFP]*	This study
VZ149	*vzEx41 [pVZ325 (Pdnj-27::dnj-27::dnj-27 3′-UTR); Punc-122::GFP]*	This study
VZ152	*vzEx42 [pVZ325 (Pdnj-27::dnj-27::dnj-27 3′-UTR); Punc-122::GFP]*	This study
VZ293	*vzEx107 [pVZ451 (Pmyo-3::dnj-27 cDNA::unc-54 3′-UTR); Ptrx-3::mCherry]*	This study
VZ294	*vzEx108 [pVZ451 (Pmyo-3::dnj-27 cDNA::unc-54 3′-UTR); Ptrx-3::mCherry]*	This study
VZ295	*vzEx109 [pVZ451 (Pmyo-3::dnj-27 cDNA::unc-54 3′-UTR); Ptrx-3::mCherry]*	This study
	ER colocalization strains[b]	
VZ254	*vzEx90 [pVZ448 (Pmyo-3::mCherry::tram-1)]*	This study
VZ255	*vzEx91 [pVZ448 (Pmyo-3::mCherry::tram-1)]*	This study
VZ256	*vzEx92 [pVZ448 (Pmyo-3::mCherry::tram-1)]*	This study
	Aβ-peptide strains	
CL647	*smg-1 (cc546ts) I; rrf-3 (pk1426) II; dvIs27 [pAF29 (Pmyo-3::Aβ 3-42::let-858 3′-UTR); pRF4 (rol-6 (su1006))] X*	This study
CL2006	*dvIs2 [pCL12 (Punc-54::Aβ 3-42::unc-54 3′-UTR); pRF4 (rol-6 (su1006))] II*	(8)
VZ158	*dvIs2 [pCL12 (Punc-54::Aβ 3-42::unc-54 3′-UTR) + pRF4 (rol-6 (su1006))] II; vzEx41 [pVZ325 (Pdnj-27::dnj-27::dnj-27 3′-UTR); Punc-122::GFP]*	This study
	α-Synuclein strains	
UA50	*baIn13 [Punc-54::α-synuclein::GFP; Punc-54::tor-2]*	(6)
NL5901	*unc-119 (ed3) III; pkIs2386 [Punc-54::α-synuclein::YFP::unc-54 3′-UTR; unc-119(+)] IV*	(12)
VZ303	*unc-119 (ed3) III; pkIs2386 [Punc-54::α-synuclein::YFP::unc-54 3′-UTR; unc-119(+)] IV; vzEx107 [pVZ451 (Pmyo-3::dnj-27 cDNA::unc-54 3′-UTR); Ptrx-3::mCherry]*	This study
UA44	*baIn11 [Pdat-1::α-synuclein::unc-54 3′-UTR; Pdat-1::GFP]*	(2)
VZ199	*baIn11 [Pdat-1::α-synuclein::unc-54 3′-UTR; Pdat-1::GFP]; vzEx41 [pVZ325 (Pdnj-27::dnj-27::3′-UTR dnj-27); Punc-122::GFP]*	This study
	polyQ strains	
AM141	*rmIs133 [Punc-54::Q40::YFP] X*	(9)
VZ299	*rmIs133 [Punc-54::Q40::YFP] X; vzEx107[pVZ451(Pmyo-3::dnj-27 cDNA::unc-54 3′-UTR); Ptrx-3::mCherry]*	This study
	Endoplasmic reticulum UPR reporter strain	
SJ4005	*zcIs4 [Phsp-4::GFP] V*	(1)
	Human ERdj5 derivative strains	
VZ314	*vzEx123 [pVZ476 (Pmyo-3::hERdj5 cDNA::unc-54 3′-UTR); Punc-122::GFP]*	This study
VZ315	*vzEx124 [pVZ476 (Pmyo-3::hERdj5 cDNA::unc-54 3′-UTR); Punc-122::GFP]*	This study
VZ316	*unc-119 (ed3) III; pkIs2386 [Punc-54::α-synuclein::YFP::unc-54 3′-UTR; unc-119(+)] IV; vzEx123 [pVZ476 (Pmyo-3::hERdj5 cDNA::unc-54 3′-UTR); Punc-122::GFP]*	This study
VZ317	*dvIs2 [pCL12 (Punc-54::Aβ 3-42::unc-54 3′-UTR); pRF4 (rol-6 (su1006))] II; vzEx123 [pVZ476 (Pmyo-3::hERdj5 cDNA::unc-54 3′-UTR); Punc-122::GFP]*	This study
VZ336	*vzEx131 [pVZ476 (Pmyo-3::hERdj5 cDNA::unc-54 3′-UTR); Pmyo-2::mCherry]*	This study
VZ337	*vzEx132 [pVZ476 (Pmyo-3::hERdj5 cDNA::unc-54 3′-UTR); Pmyo-2::mCherry]*	This study
VZ338	*vzEx133 [pVZ476 (Pmyo-3::hERdj5 cDNA::unc-54 3′-UTR); Pmyo-2::mCherry]*	This study
VZ361	*rmIs133 [Punc-54::Q40::YFP] X; vzEx131 [pVZ476 (Pmyo-3::hERdj5 cDNA::unc-54 3′-UTR); Pmyo-2::mCherry]*	This study
VZ362	*rmIs133 [Punc-54::Q40::YFP] X; vzEx132 [pVZ476 (Pmyo-3::hERdj5 cDNA::unc-54 3′-UTR); Pmyo-2::mCherry]*	This study
VZ363	*rmIs133 [Punc-54::Q40::YFP] X; vzEx133 [pVZ476 (Pmyo-3::hERdj5 cDNA::unc-54 3′-UTR); Pmyo-2::mCherry]*	This study
	Muscle cytoplasmic degradation strains	
PD55	*tra-3 (e1107) IV; ccIs55 [sup-7 (st5); Punc-54::unc-54::lacZ] V*	(13)
PJ1009	*unc-51 (e369) V; ccIs55 [sup-7 (st5); Punc-54::unc-54::lacZ] V*	(10)
PJ1103	*mpk-1 (n2521) III; cha-1(1182ts) IV; him-8 (e1489) V; ccIs55 [sup-7 (st5); Punc-54::unc-54::lacZ] V*	(11)
PJ1132	*daf-18 (e1375) IV; ccIs55 [sup-7 (st5); Punc-54::unc-54::lacZ] V*	(10)
PJ1288	*ced-3(n717) IV; ccIs55 [sup-7 (st5); Punc-54::unc-54::lacZ] V*	(3)

(*continued*)

Supplementary Table S1. (Continued)

Strain name	*Genotype*	*Reference/source*
CB5600	*ccIs4251 [Pmyo-3::nuclearGFP::lacZ; Pmyo-3::mitoGFP] I; him-8 (e1489) IV*	(4)
PJ727	*jIs01 [Pmyo-3::myo-3::GFP; rol-6 (su1006)]; ccIs55 [sup-7 (st5); Punc-54::unc-54::lacZ] V*	(5)
	Mitochondrial fragmentation strains	
PS6187	*unc-119 (ed3) III; syEx1155 [Pmyo-3::tomm-20::mRFP::3xMyc; pPD#16b (unc-119+)]*	Amir Sapir and Paul Sternberg gift
VZ272	*dvIs2 [pCL12 (Punc-54::Aβ 3-42::unc-54 3′-UTR); pRF4 (rol-6 (su1006))] II; syEx1155 [Pmyo-3::tomm-20::mRFP::3xMyc; pPD#16b (unc-119+)]*	This study
VZ418	*unc-119 (ed3) III; pkIs2386 [Punc-54::α-synuclein::YFP::unc-54 3′-UTR; unc-119(+)] IV; syEx1155 [Pmyo-3::tomm-20::mRFP::3xMyc; pPD#16b (unc-119+)]*	This study
VZ421	*rmIs133 [Punc-54::Q40::YFP] X; syEx1155 [Pmyo-3::tomm-20::mRFP::3xMyc; pPD#16b (unc-119+)]*	This study
VZ430	*pkIs2386 [Punc-54::α-synuclein::YFP, unc-119(+)] IV; syEx1155 [Pmyo-3::tomm-20::mRFP::3xMyc; pPD#16b(unc-119+)]; vzEx41 [pVZ325 (Pdnj-27::dnj-27::3′-UTR dnj-27); p225 (Punc-122::GFP)]*	This study
VZ431	*dvIs2 [pCL12 (Punc-54::Aβ 3-42::unc-54 3′-UTR); pRF4 (rol-6 (su1006))] II; syEx1155 [Pmyo-3::tomm-20::mRFP::3xMyc; pPD#16b(unc-119+)]; vzEx41 [pVZ325 (Pdnj-27::dnj-27::3′-UTR dnj-27); p225 (Punc-122::GFP)]*	This study

[a]CGC, *Caenorhabditis* Genetics Center (http://cbs.umn.edu/CGC/).

[b]The strains VZ184 and VZ254 were crossed to generate strains of genotype: *vzEx60 [pVZ378 (Pdnj-27::dnj-27::YFP::KDEL)]; vzEx90 [pVZ448 (Pmyo-3::mCherry::TRAM-1)].* However, this strain produced no viable double transgenic progeny. Therefore, we demonstrated endoplasmic reticulum colocalization in the F1 double transgenic generation.

cDNA, complementary DNA; ER, endoplasmic reticulum; GFP, green fluorescent protein; polyQ, polyglutamine; UPR, unfolded protein response; UTR, untranslated region; YFP, yellow fluorescent protein.

Supplementary Table S2. Effect of RNAi Downregulation of *Caenorhabditis elegans* Genes Encoding for Thioredoxins (with the Conserved Active Site Sequence WCGPC) and Thioredoxin Reductases on the Paralysis of Aβ Worms and the Aggregation of α-syn::GFP

Gene name	*Gene sequence designation*	*Aβ dependent paralysis (CL647)*	*α-syn::GFP aggregation (UA50)*
trxr-1	*C06G3.7*	Increases paralysis	No effect
trxr-2	*ZK637.10*	Increases paralysis	No effect
trx-1	*B0228.5*	Decreases paralysis	No effect
trx-2	*B0024.9*	No effect	No effect
trx-3	*M01H9.1*	Increases paralysis	No effect
trx-4	*Y44E3A.3*	No effect	No effect
trx-5	*K02H11.6*	No effect	No effect
txl	*Y54E10A.3*	No effect	No effect
dnj-27	*Y47H9C.5*	Increases paralysis	Increases aggregation

α-syn, alpha-synuclein; Aβ, beta amyloid peptide; RNAi, RNA interference.